EDGE ARTICLE

Check for updates

Realizing high hydrogen evolution activity under visible light using narrow band gap organic photocatalysts†

Changzhi Han,[a] Peihua Dong,[a] Haoran Tang,[b] Peiyun Zheng,[a] Chong Zhang,*[a] Feng Wang, [c] Fei Huang [b] and Jia-Xing Jiang [a]

The design and synthesis of conjugated semiconducting polymers for photocatalytic hydrogen evolution have engendered intense recent interest. However, most reported organic polymer photocatalysts show a relatively broad band gap with weak light absorption ability in the visible light region, which commonly leads to a low photocatalytic activity under visible light. Herein, we synthesize three novel dithieno[3,2-*b*:2′,3′-*d*]thiophene-*S*,*S*-dioxide (DTDO) containing conjugated polymer photocatalysts by a facile C−H arylation coupling polymerization reaction. The resulting polymers show a broad visible light absorption range up to 700 nm and a narrow band gap down to 1.81 eV due to the introduction of the DTDO unit. Benefiting from the donor−acceptor polymer structure and the high content of the DTDO unit, the three-dimensional polymer PyDTDO-3 without the addition of a Pt co-catalyst shows an attractive photocatalytic hydrogen evolution rate of 16.32 mmol h^{-1} g^{-1} under visible light irradiation, which is much higher than that of most reported organic polymer photocatalysts under visible light.

Introduction

The utilization of sunlight to generate hydrogen from water has been considered as a facile and cost-effective technology for the conversion of solar energy to chemical energy.[1–3] The past few decades have witnessed great progress of inorganic semiconducting photocatalysts,[4,5] while most inorganic photocatalysts show poor photocatalytic activity under visible light. Recently, conjugated organic semiconductors have attracted much attention as photocatalysts for hydrogen generation because of their potential advantages such as a flexible molecular structure and tuneable electronic properties and band gaps.[6–12] Representative organic polymer photocatalysts mainly include linear conjugated polymers (CPs),[13–19] graphitic carbon nitrides (g-C$_3$N$_4$),[20,21] conjugated microporous polymers

(CMPs),[22–27] crystalline covalent organic frameworks (COFs),[28–33] and covalent triazine-based frameworks (CTFs).[34–39]

It has been proved that the selectivity of a suitable building block is important to improve the photocatalytic activity of organic polymer photocatalysts, and many studies have demonstrated that dibenzothiophene-*S*,*S*-dioxide with strong electron accepting ability is an efficient building block to generate organic polymer photocatalysts with high photocatalytic activity.[18,40–43] For example, the dibenzothiophene-*S*,*S*-dioxide-containing covalent organic framework FS-COF exhibited a hydrogen evolution rate (HER) of 10.1 mmol h^{-1} g^{-1} under visible light.[41] A dibenzothiophene-*S*,*S*-dioxide-containing conjugated microporous polymer of PyDF with fluorine atoms showed a higher HER of 18.93 mmol h^{-1} g^{-1} under UV-Vis light illumination.[44] A triazine-Ph-CPP polymer consisting of 1,3,5-triazine and dibenzothiophene-*S*,*S*-dioxide building blocks exhibited an excellent HER of 16.28 mmol h^{-1} g^{-1} upon broadband light irradiation.[45] However, most reported organic polymer photocatalysts show a relatively broad band gap and weak light absorption ability in the visible light region, which commonly leads to their low photocatalytic activity under visible light. Therefore, it is highly desirable to develop organic polymer photocatalysts with a broad visible light absorption range to efficiently utilize visible light of sunlight.

In this study, we designed and synthesized three novel conjugated polymer photocatalysts with a narrow band gap by integrating the dithieno[3,2-*b*:2′,3′-*d*]thiophene-*S*,*S*-dioxide (DTDO) unit into a one-dimensional (1D) linear polymer backbone and three-dimensional (3D) polymer skeleton. The

[a] Key Laboratory for Macromolecular Science of Shaanxi Province, Shaanxi Engineering Laboratory for Advanced Energy Technology, School of Materials Science and Engineering, Shaanxi Normal University, Xi'an, Shaanxi 710062, P. R. China. E-mail: chongzhangabc@snnu.edu.cn; jiaxing@snnu.edu.cn

[b] Institute of Polymer Optoelectronic Materials and Devices, State Key Laboratory of Luminescent Materials and Devices, South China University of Technology, Guangzhou, 510641, China

[c] Key Laboratory for Green Chemical Process of Ministry of Education, School of Chemical Engineering and Pharmacy, Wuhan Institute of Technology, Wuhan 430073, P. R. China

† Electronic supplementary information (ESI) available: Details for the synthesis and characterization of the polymers, PXRD patterns, SEM images, CV curves, and DFT simulations. See DOI: 10.1039/d0sc05866a

introduction of the DTDO unit with a narrow band gap and strong electron-withdrawing ability extends the light absorption range and thus enhances the visible light absorption ability of the resulting polymers. In addition, the donor–acceptor (D–A) polymer structure promotes the separation of light-induced charge carriers. Benefiting from the high hydrophilicity, broad light absorption and the high DTDO content with plentiful available active sites, the 3D polymer **PyDTDO-3** exhibits an attractive photocatalytic HER of 16.32 mmol h^{-1} g^{-1} under visible light irradiation.

Results and discussion

The three newly designed polymers were synthesized by a direct C–H arylation coupling polymerization reaction from dithieno [3,2-b:2′,3′-d]thiophene-S,S-dioxide and 2,7-dibromopyrene, 1,6-dibromopyrene or 1,3,6,8-tetrabromopyrene (Scheme 1). The resulting polymers were obtained as brownish yellow (for **PyDTDO-1**), red (for **PyDTDO-2**), and deep-red (**PyDTDO-3**) insoluble powder. The insoluble nature of the polymers could be attributed to their rigid aromatic skeletons. The chemical structure of the polymers was confirmed by Fourier-transform infrared (FT-IR) spectroscopy and solid-state ^{13}C NMR measurements. The FT-IR spectra of the polymers showed the characteristic stretching vibration bands of the sulphone group (O=S=O) at around 1312 and 1138 cm^{-1},[42,45] the stretching vibration of the thiophene ring at around 1470 cm^{-1} and the typical stretching vibration band of aromatic skeletons at around 1601 cm^{-1} (Fig. 1a). Fig. 1b shows the solid-state ^{13}C NMR spectra and the assignment of carbons for the polymers. The signal of the characteristic carbon bonded to the sulphone group was observed at around 124 ppm. Thermogravimetric analysis revealed that all polymers have moderate thermal stability with a decomposition temperature at around 300 °C in a nitrogen atmosphere (Fig. 1c), while **PyDTDO-1** and **PyDTDO-2** show a higher thermal stability than **PyDTDO-3**, possibly due to the higher polymerization degree. The powder X-ray diffraction profiles showed that the linear polymers **PyDTDO-1** and
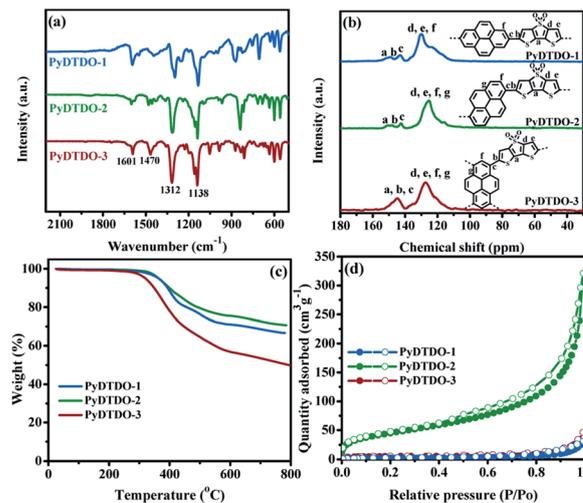

Fig. 1 (a) FT-IR spectra of the polymers; (b) the solid-state ^{13}C CP-MAS NMR spectra and the assignment of carbons for the polymers; (c) thermogravimetric analysis traces of the polymers under a nitrogen atmosphere; (d) nitrogen adsorption/desorption isotherms of the polymers.

PyDTDO-2 have some crystalline structures due to the π–π stacking interaction between the 1D polymer chains (Fig. S1†).

The nitrogen adsorption and desorption measurement demonstrated that the three polymers show a type IV nitrogen gas sorption character with a sharp nitrogen adsorption at high relative pressure (Fig. 1d), indicative of some meso/macropores in the sample due to the formation of voids among the nanosphere particles. Compared to **PyDTDO-1**, **PyDTDO-2** shows a higher specific surface area of 151 m^2 g^{-1}, possibly due to the twisted polymer structure leading to porosity among the linear polymer chains. The low specific surface area of 40 m^2 g^{-1} for the cross-linked polymer **PyDTDO-3** could be attributed to the large steric hindrance and the low reactivities of the monomers in this polymerization, leading to the incomplete polymerization reaction and thus the low cross-linking degree for the resulting polymer. The insoluble nature in common organic solvents of **PyDTDO-3** due to its cross-linked structure and rigid aromatic skeleton hinders the measurement of its molecular weight. The incomplete polymerization reaction was also verified from the energy dispersive X-ray spectroscopy (EDX) spectra showing the high content of the unreacted Br end group for the polymers, particularly for **PyDTDO-3** (Fig. 2a–c).

The SEM images revealed that **PyDTDO-1** and **PyDTDO-2** have a flake-like morphology, while **PyDTDO-3** shows a nano-particle-aggregated layer morphology (Fig. 2d–f and S2†). Contact angle measurement was performed to evaluate the water wettability of the polymers. The contact angles of **PyDTDO-1**, **PyDTDO-2** and **PyDTDO-3** were found to be 83.0°, 88.9°, and 63.5°, respectively (Fig. 2g–i). Compared with that of **PyDTDO-1** and **PyDTDO-2**, the higher hydrophilicity of **PyDTDO-3** can be attributed to its higher DTDO content with a polar group in the cross-linked structure, which agrees well with the EDX spectra. This is also supported by the elemental analysis result, which demonstrates a higher sulphur content of
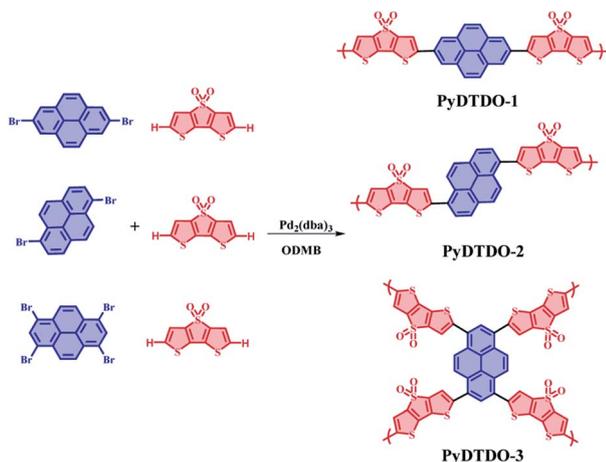
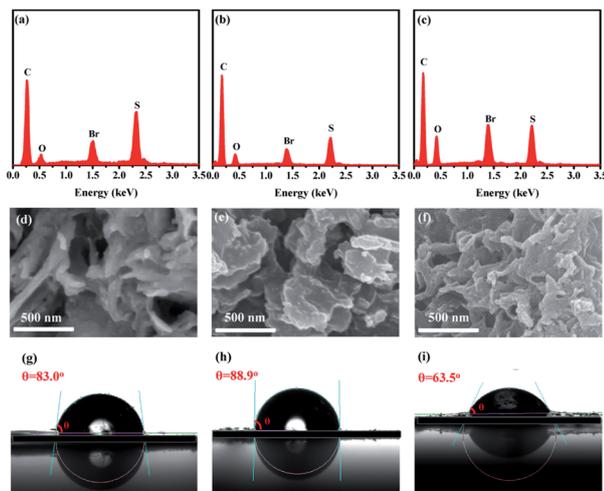Scheme 1 The synthetic routes for the polymers.

Fig. 2 EDX spectra of PyDTDO-1 (a), PyDTDO-2 (b) and PyDTDO-3 (c); SEM images of PyDTDO-1 (d), PyDTDO-2 (e) and PyDTDO-3 (f); optical photos of H_2O on the surfaces of PyDTDO-1 (g), PyDTDO-2 (h) and PyDTDO-3 (i) with the contact angles.

Fig. 3 (a) UV/Vis reflectance spectra of the polymers; (b) Tauc plots of the Kubelka−Munk function vs. energy; (c) PL spectra of the polymers (inset: photographs of the polymers under UV light); (d) photo-luminescence decay traces of the polymers. (e) Energy band positions. (f) Photocurrent curves of the polymers.

20.10% in PyDTDO-3 than PyDTDO-1 (12.37%) and PyDTDO-2 (13.95%). The high hydrophilicity of PyDTDO-3 will facilitate the adsorption of water molecules on the polymer surface, thus leading to high photocatalytic activity.

The optical properties of the polymers were investigated by UV/Vis diffuse reflectance and photoluminescence (PL) emission spectroscopy using the solid-state polymer powder. The UV/Vis reflectance spectra revealed that all the polymers exhibit a broad UV/Vis absorption range from 300 to 700 nm (Fig. 3a). More importantly, an obvious red-shift tendency in the light absorption range was observed from PyDTDO-1 to PyDTDO-2 and to PyDTDO-3, which could be attributed to the orderly extended conjugation degree, since the 1,6-linkage pattern on pyrene generates much more orbital overlap between pyrene and DTDO units for the electron delocalization than the 2,7-linkage pattern, and the 1,3,6,8-tetralinkage pattern with a cross-linked structure leads to more orbital overlap in PyDTDO-3.[46,47] Meanwhile, the higher content of the DTDO unit with a narrow band gap should be another factor that endows PyDTDO-3 with broader light absorption than PyDTDO-1 and PyDTDO-2. As a result, PyDTDO-3 shows a smaller band gap of 1.81 eV than PyDTDO-1 (2.07 eV) and PyDTDO-2 (1.92 eV) (Fig. 3b). The band gap for PyDTDO-3 is also smaller than that of most reported organic polymer photocatalysts.[36,48,49] All three polymers exhibit weak solid state photoluminescence emission under UV light, while PyDTDO-3 shows an obvious red-shift in the PL emission peak compared to PyDTDO-1 and PyDTDO-2 (Fig. 3c), further demonstrating its narrower band gap. As revealed by the time-resolved fluorescence decay spectra (Fig. 3d), PyDTDO-3 exhibits a shorter excited state lifetime ($\tau 1$ = 0.6912 ns) than PyDTDO-1 ($\tau 1$ = 0.8449 ns) and PyDTDO-2 ($\tau 1$ = 0.9851 ns) (Table S1†), implying a lower inactivation possibility of photo-induced excited state electrons in PyDTDO-3. Cyclic voltammetry measurement combined with UV/Vis spectra was employed to study the band positions of the
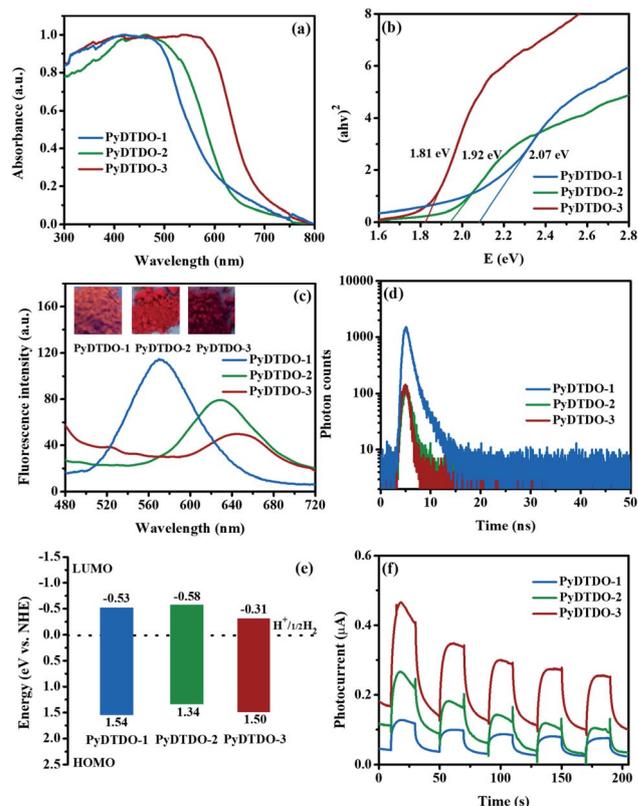
polymers (Fig. S3†). Owing to the similar chemical structure, no obvious difference was observed in the lowest unoccupied molecular orbital (LUMO) energy level for the two linear polymers PyDTDO-1 and PyDTDO-2, while all the polymers showed a high enough LUMO energy level to drive the half-reaction of hydrogen evolution (Fig. 3e). The lower LUMO level of PyDTDO-3 than PyDTDO-1 and PyDTDO-2 can be ascribed to the higher content of electron acceptor DTDO. The photocurrent test demonstrated that the current response sharply increased from PyDTDO-1 to PyDTDO-3 under UV/Vis light irradiation (Fig. 3f), implying that more photo-induced charge carriers could be produced by PyDTDO-3, which is beneficial for the photo-catalytic hydrogen evolution reaction.

Density functional theory (DFT) calculations revealed that all the polymers have an obvious separation of HOMO and LUMO orbitals (Fig. 4), a typical feature of D–A polymers, due to the electron-donating ability of the pyrene unit and the strong electron-withdrawing effect of the DTDO unit. In addition, the 1D polymer PyDTDO-2 and 3D polymer PyDTDO-3 have a higher degree of electron delocalization than PyDTDO-1. The dihedral angles calculated using DFT for the three polymers do not follow the same trend of the simulated orbital distribution as shown in Fig. 4, demonstrating that the electron delocalization depends on more linking patterns than dihedral angles
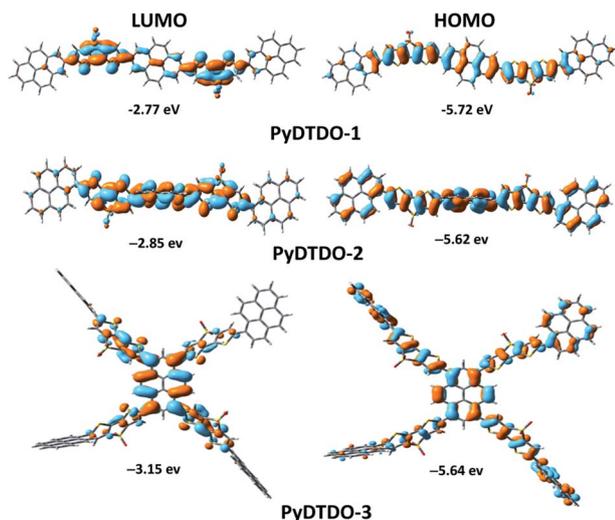
Fig. 4 HOMO and LUMO orbital distribution of the polymers from DFT calculations.

(Fig. S4†). The enhanced electron delocalization and expanded LUMO orbital distribution, particularly for **PyDTDO-3**, will provide plentiful photocatalytically active sites for the reduction reaction of water.

The photocatalytic hydrogen evolution experiment was carried out by using the bare polymer (10 mg) suspension in deionized water and ascorbic acid (AA) as the sacrificial hole-scavenger. As shown in Fig. 5a, all polymers show high photocatalytic activity under the simulated solar light irradiation. The amount of the produced hydrogen shows almost a linear increase with the photocatalytic reaction time, indicating the excellent photocatalytic stability. Among the three polymers, the cross-linked polymer **PyDTDO-3** shows the highest

Fig. 5 (a) Hydrogen generation as a function of reaction time of the bare polymers (10 mg) under UV/Vis light ($\lambda > 300$ nm), and (b) visible light ($\lambda > 420$ nm); (c) stability test of **PyDTDO-3** in a 1.0 M aqueous solution of AA containing 10 vol% DMF under visible light ($\lambda > 420$ nm); (d) the AQY plots and UV/Vis reflectance spectrum of **PyDTDO-3**.

photocatalytic activity with an average HER of 24.97 mmol h^{-1} g^{-1} under UV/Vis light irradiation, followed by **PyDTDO-2** (7.05 mmol h^{-1} g^{-1}) and then **PyDTDO-1** (5.67 mmol h^{-1} g^{-1}). More importantly, all the polymers show an attractive photocatalytic activity under visible light irradiation ($\lambda > 420$ nm) (Fig. 5b). In particular, an impressive HER of 16.32 mmol h^{-1} g^{-1} was obtained by the bare **PyDTDO-3** without addition of a Pt co-catalyst, which is much higher than that of **PyDTDO-1** (1.91 mmol h^{-1} g^{-1}) and **PyDTDO-2** (3.67 mmol h^{-1} g^{-1}). Compared to that of **PyDTDO-1** and **PyDTDO-2**, the higher photocatalytic activity of **PyDTDO-3** can be ascribed to its broader visible light absorption range and higher hydrophilicity. In addition, the higher content of DTDO species distributed along the 3D polymer skeletons in **PyDTDO-3** could provide many more available active sites for the photocatalytic hydrogen evolution reaction compared with the lower DTDO content of **PyDTDO-1** and **PyDTDO-2**.

Some previous research studies demonstrated that the residual Pd in polymer photocatalysts produced from Pd-catalyzed polymerization might contribute to the H_2 production.[50,51] As shown in Fig. 2a–c, no any Pd signal could be observed in all of the polymers by the EDX measurement, which might be attributed to the low content of Pd in the three polymers. This is also evidenced by inductively coupled plasma atomic emission spectroscopy (ICP-MS), which demonstrates that the content of Pd is 62, 78 and 16 ppm for **PyDTDO-1**, **PyDTDO-2** and **PyDTDO-3**, respectively (Fig. S5†). In addition, no any direct relationship could be obtained between the residual Pd content and the photocatalytic hydrogen performance. For instance, **PyDTDO-2** shows the highest Pd content among the resulting polymers, while **PyDTDO-3** exhibits the highest hydrogen evolution rate, demonstrating that the residual Pd has no significant effect on the photocatalytic activity in these polymer photocatalysts, which is probably due to the low Pd content, as observed in other CMP photocatalysts.[42,44]

To investigate the influence of the sacrificial reagents on the photocatalytic performance of the polymers, we also evaluated the photocatalytic activity of **PyDTDO-3** using triethylamine (TEA) and triethanolamine (TEOA) as the sacrificial reagents. The HER values are 0.56 mmol h^{-1} g^{-1} for TEA and 1.23 mmol h^{-1} g^{-1} for TEOA under visible light; both are lower than the value of 16.32 mmol h^{-1} g^{-1} when AA is used as the sacrificial reagent (Fig. S6†). Similar results were also observed in many other organic polymer photocatalysts.[9,48,52] This could be attributed to that the different sacrificial reagents lead to different pH values, e.g., pH = 2.53, 12.16 and 10.57 in AA, TEA and TEOA, respectively, corresponding to the potentials for the proton reduction of −0.149, −0.717 and −0.624, based on the Nernst equation $E(H^+/H_2) = -0.059 \times pH$. The higher potential of H^+/H_2 in AA solution indicates a stronger driving force between the polymer photocatalysts and the water reduction.[41,52,53] Therefore, a higher photocatalytic activity was achieved when using AA as the sacrificial reagent.

It should be noted that the visible light activity of bare **PyDTDO-3** is comparable with that of state-of-the-art organic polymer photocatalysts (Table S2†). In particular, the HER of
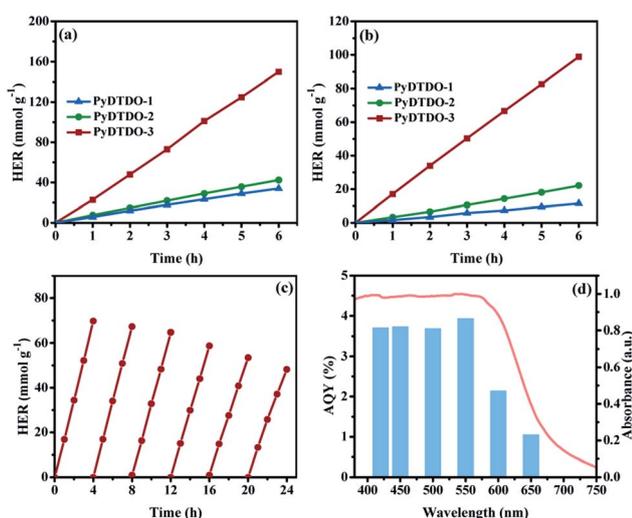
16.32 mmol h^{-1} g^{-1} is also higher than that of most dibenzothiophene-*S*,*S*-dioxide based polymer photocatalysts under visible light (λ > 420 nm), such as the linear polymers P7 (3.68 mmol h^{-1} g^{-1})[40] and P7-E (6.02 mmol h^{-1} g^{-1}),[17] the conjugated microporous polymer PyDOBT-1 (5.70 mmol h^{-1} g^{-1}),[54] the covalent organic framework FS-COF (10.10 mmol h^{-1} g^{-1}),[41] and the triazine-containing polymer triazine-Ph-CPP with dibenzothiophene-*S*,*S*-dioxide (3.50 mmol h^{-1} g^{-1}).[45] We need to point out that the direct comparison of the HERs from different data sets might be difficult due to the variations in the photocatalytic reaction setup.[22,55] However, the high visible light activity of the DTDO-containing polymer **PyDTDO-3** should be related to its broad light absorption range as well the strong light absorption ability in the visible light region from 400 to 600 nm, which enhance the utilization of visible light.

PyDTDO-3 shows a slight decrease in the photocatalytic activity during a continuous photocatalytic experiment for 24 h (Fig. 5c), demonstrating the moderate long-term photocatalytic stability of the polymer photocatalyst. The apparent quantum yield (AQY) of **PyDTDO-3** (10 mg) was found as a function of the wavelength of the incident light (Fig. 5d). The AQYs were measured to be 3.70, 3.73, 3.68 and 3.93% at 420, 450, 500, and 550 nm, respectively. The very close AQY at these wavelengths is well in line with the UV/Vis reflectance spectrum of **PyDTDO-3**, which shows a relatively flat curve with similar absorption ability in this spectral range. With further increase in the incident light wavelength, the AQY decreases to 2.14% at 600 nm, and 1.05% at 650 nm, which could be attributed to the weak light absorption ability of **PyDTDO-3** at these wavelengths as shown in Fig. 5d.

We also synthesized the other two batches of **PyDTDO-3** under the same polymerization conditions in order to test the repeatability of the polymer photocatalyst. The photocatalytic hydrogen evolution experiment revealed that the batch-to-batch polymers have very similar photocatalytic activity with a slight difference in the photocatalytic hydrogen evolution rate (Fig. 6a), indicative of the excellent reproducibility of the DTDO-containing polymer photocatalysts. To test the structural stability of the polymers for the photocatalytic reaction, the collected sample of **PyDTDO-3** after the 24 h photocatalytic reaction was washed with water and tetrahydrofuran and characterized by FT-IR, solid-state ^{13}C NMR, UV/Vis and PL

measurements (Fig. S7–S10†). No obvious change in the polymer structures and physical properties was observed for the recovered samples, implying the outstanding structural stability of the polymers along the long-term photocatalytic reaction. However, the FT-IR spectrum for the recovered sample of **PyDTDO-3** showed the characteristic peaks of ascorbic acid (Fig. 6b), which are absent in the recovered samples of **PyDTDO-1** and **PyDTDO-2** (Fig. S10†). This could be attributed to the physisorbed ascorbic acid molecules in **PyDTDO-3** since the 3D cross-linked polymer structure and high DTDO content with high hydrophilicity enhanced the interaction between the polymer and ascorbic acid molecules. The high hydrophilicity is beneficial for the adsorption of water molecules on the surface of **PyDTDO-3**, and the physisorbed ascorbic acid molecule promotes the capture of photo-induced holes. As a result, **PyDTDO-3** shows a much higher photocatalytic activity than **PyDTDO-1** and **PyDTDO-2**.

Conclusions

In summary, three novel DTDO-containing conjugated polymer photocatalysts were developed by direct C–H arylation coupling polymerization. All polymers show narrow band gaps with a broad visible light absorption range up to 700 nm due to the introduction of the DTDO unit. The conjugated skeleton and the donor–acceptor polymer structure promote the transmission and separation of photo-induced electron/hole pairs. The high DTDO content enhances the hydrophilicity of the polymer and provides more available active sites for the photocatalytic hydrogen evolution reaction. The cross-linked structure with the 1,3,6,8-tetralinkage leads to high conjugation along the polymer chains with expanded LUMO orbital distribution. As a result, the bare 3D polymer **PyDTDO-3** shows an attractive HER of 16.32 mmol h^{-1} g^{-1} under visible light irradiation, demonstrating that it is an efficient approach to improve the photocatalytic activity of organic polymers under visible light by integrating a narrow band gap unit into a conjugated polymer skeleton.

Experimental

Chemicals

All chemicals employed in this work were obtained from J&K Scientific Ltd or Sigma-Aldrich. Pivalic acid (PivOH), ascorbic acid, anhydrous potassium carbonate (K$_2$CO$_3$), anhydrous 1,2-dimethylbenzene (ODMB), tris(dibenzylideneacetone)dipalladium (Pd$_2$(dba)$_3$), tris(2-methoxyphenyl)phosphine (P(*o*-MeOPh)$_3$), 1,6-dibromopyrene, 2,7-dibromopyrene, and *N*,*N*-dimethylformamide (DMF) were used as received without further purification. 1,3,6,8-Tetrabromopyrene was prepared according to the reported literature.[56] The polymers were synthesized by a modified method reported previously.[57]

Synthesis of conjugated polymer PyDTDO-1. Under N$_2$ protection, 5 mL anhydrous ODMB was added into a mixture of dithieno[3,2-*b*:2′,3′-*d*]thiophene-*S*,*S*-dioxide (114.2 mg, 0.5 mmol), 2,7-dibromopyrene (180.0 mg, 0.5 mmol), anhydrous K$_2$CO$_3$ (207.3 mg, 1.5 mmol), Pd$_2$(dba)$_3$ (13.7 mg, 0.015 mmol), PivOH (30.64 mg, 0.3 mmol) and P(*o*-MeOPh)$_3$ (10.6 mg, 0.03
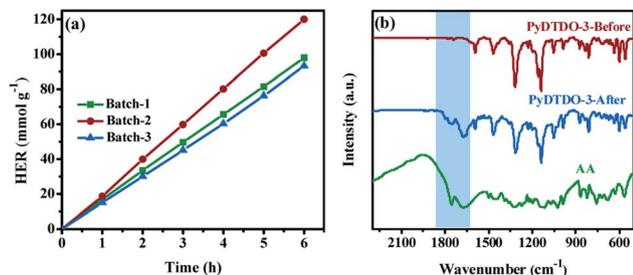

Fig. 6 (a) Hydrogen generation as a function of reaction time of **PyDTDO-3** from different batches (10 mg) under visible light (λ > 420 nm); (b) FT-IR spectra of **PyDTDO-3** before and after the photocatalytic reaction under visible light for 24 h in a mixture of AA/DMF/water.

mmol). The reaction mixture was heated to 100 °C and stirred for 72 h. After cooling to room temperature, the precipitate was obtained by filtration. The resulting polymer was washed successively with methanol, deionized water and dichloromethane (100 mL for each), respectively. After drying in a vacuum at 100 °C for 24 h, the polymer **PyDTDO-1** was obtained as brownish yellow powder (yield: 83.2%). Anal. calcd for $(C_{24}H_{10}O_2S_3)_n$ (%): C 67.58; H 2.36; S 22.55. Found: C 65.11; H 2.52; S 12.37.

Synthesis of conjugated polymer PyDTDO-2. Dithieno[3,2-b:2′,3′-d]thiophene-S,S-dioxide (114.2 mg, 0.5 mmol), 1,6-dibromopyrene (180.0 mg, 0.5 mmol), anhydrous K_2CO_3 (207.3 mg, 1.5 mmol), $Pd_2(dba)_3$ (13.7 mg, 0.015 mmol), PivOH (30.64 mg, 0.3 mmol) and P(o-MeOPh)$_3$ (10.6 mg, 0.03 mmol) were used in this polymerization. The polymer **PyDTDO-2** was obtained as red powder (yield: 80.4%). Anal. calcd for $(C_{24}H_{10}O_2S_3)_n$ (%): C 67.58; H 2.36; S 22.55. Found: C 62.11; H 2.82; S 13.95.

Synthesis of conjugated polymer PyDTDO-3. Dithieno[3,2-b:2′,3′-d]thiophene-S,S-dioxide (114.2 mg, 0.5 mmol), 1,3,6,8-tetrabromopyrene (129.4 mg, 0.25 mmol), anhydrous K_2CO_3 (207.3 mg, 1.5 mmol), $Pd_2(dba)_3$ (13.7 mg, 0.015 mmol), PivOH (30.64 mg, 0.3 mmol) and P(o-MeOPh)$_3$ (10.6 mg, 0.03 mmol) were used in this polymerization. The polymer **PyDTDO-3** was obtained as deep-red powder (yield: 85.4%). Anal. calcd for $(C_{32}H_{10}O_4S_6)_n$ (%): C 59.06; H 1.55; S 29.56. Found: C 54.40; H 3.28; S 20.10.

Photocatalytic hydrogen generation experiment

The photocatalytic hydrogen generation experiments of the photocatalysts were performed on a set of photocatalytic equipment (Beijing Perfect Light Co.). First of all, 10 mg of the as-synthesized polymer and ascorbic acid as a sacrificial reagent were ultrasonically dispersed in a mixed solution containing 90 mL water and 10 mL N,N-dimethylformamide as a dispersant to form a well-dispersed polymer suspension, and the concentration of ascorbic acid was 1.0 M. After the photocatalytic system was degassed to remove the dissolved air, the suspension was irradiated with a 300 W Xe lamp in a vacuum with stirring. Circulating cooling water was used to maintain the photocatalytic reaction temperature at 6 °C. A 420 nm filter was used to filter off ultraviolet light to obtain simulated visible light irradiation ($\lambda > 420$ nm). The produced hydrogen was measured online by using a gas chromatograph. The details of the photocatalytic experiments using triethylamine and triethanolamine as the sacrificial reagents are provided in the ESI.†

Conflicts of interest

There are no conflicts to declare.

Acknowledgements

Notes and references

1 K. Maeda and K. Domen, *J. Phys. Chem. Lett.*, 2010, **1**, 2655–2661.
2 Z. Wang, C. Li and K. Domen, *Chem. Soc. Rev.*, 2019, **48**, 2109–2125.
3 J. Jayakumar and H. H. Chou, *ChemCatChem*, 2020, **12**, 689–704.
4 A. Fujishima and K. Honda, *Nature*, 1972, **238**, 37–38.
5 S. Chandrasekaran, L. Yao, L. Deng, C. Bowen, Y. Zhang, S. Chen, Z. Lin, F. Peng and P. Zhang, *Chem. Soc. Rev.*, 2019, **48**, 4178–4280.
6 Y. Wang, A. Vogel, M. Sachs, R. S. Sprick, L. Wilbraham, S. J. A. Moniz, R. Godin, M. A. Zwijnenburg, J. R. Durrant, A. I. Cooper and J. Tang, *Nat. Energy.*, 2019, **4**, 746–760.
7 L. Y. Ting, J. Jayakumar, C. L. Chang, W. C. Lin, M. H. Elsayed and H. H. Chou, *J. Mater. Chem. A*, 2019, **7**, 22924–22929.
8 C. Zhao, Z. Chen, R. Shi, X. Yang and T. Zhang, *Adv. Mater.*, 2020, **32**, 1907296.
9 J. Kosco, M. Bidwell, H. Cha, T. Martin, C. T. Howells, M. Sachs, D. H. Anjum, S. Gonzalez Lopez, L. Zou, A. Wadsworth, W. Zhang, L. Zhang, J. Tellam, R. Sougrat, F. Laquai, D. M. DeLongchamp, J. R. Durrant and I. McCulloch, *Nat. Mater.*, 2020, **19**, 559–565.
10 M. H. Elsayed, J. Jayakumar, M. Abdellah, T. H. Mansoure, K. Zheng, A. M. Elewa, C. L. Chang, L. Y. Ting, W. C. Lin, H. h. Yu, W. H. Wang, C. C. Chung and H. H. Chou, *Appl. Catal. B.*, 2020, 119659.
11 C. L. Chang, W. C. Lin, C. Y. Jia, L. Y. Ting, J. Jayakumar, M. H. Elsayed, Y. Q. Yang, Y. H. Chan, W. S. Wang, C. Y. Lu, P. Y. Chen and H. H. Chou, *Appl. Catal. B.*, 2020, **268**, 118436.
12 W. H. Wang, L. Y. Ting, J. Jayakumar, C. L. Chang, W. C. Lin, C. C. Chung, M. H. Elsayed, C. Y. Lu, A. M. Elewa and H. H. Chou, *Sustain. Energy Fuels.*, 2020, **4**, 5264–5270.
13 S. Yanagida, A. Kabumoto, K. Mizumoto, C. Pac and K. Yoshino, *J. Chem. Soc., Chem. Commun.*, 1985, **8**, 474–475.
14 P. J. Tseng, C. L. Chang, Y. H. Chan, L. Y. Ting, P. Y. Chen, C. H. Liao, M. L. Tsai and H. H. Chou, *ACS Catal.*, 2018, **8**, 7766–7772.
15 R. S. Sprick, L. Wilbraham, Y. Bai, P. Guiglion, A. Monti, R. Clowes, A. I. Cooper and M. A. Zwijnenburg, *Chem. Mater.*, 2018, **30**, 5733–5742.
16 M. Sachs, R. S. Sprick, D. Pearce, S. A. J. Hillman, A. Monti, A. A. Y. Guilbert, N. J. Brownbill, S. Dimitrov, X. Shi, F. Blanc, M. A. Zwijnenburg, J. Nelson, J. R. Durrant and A. I. Cooper, *Nat. Commun.*, 2018, **9**, 4968.
17 X. H. Zhang, X. P. Wang, J. Xiao, S. Y. Wang, D. K. Huang, X. Ding, Y. G. Xiang and H. Chen, *J. Catal.*, 2017, **350**, 64–71.
18 W. C. Lin, M. H. Elsayed, J. Jayakumar, L. Y. Ting, C. L. Chang, A. M. Elewa, W. S. Wang, C. C. Chung, C. Y. Lu and H. H. Chou, *Int. J. Hydrog. Energy.*, 2020, **45**, 32072–32081.
19 G. Shu, Y. Li, Z. Wang, J. X. Jiang and F. Wang, *Appl. Catal. B.*, 2020, **261**, 118230.

20 X. Wang, K. Maeda, A. Thomas, K. Takanabe, G. Xin, J. M. Carlsson, K. Domen and M. Antonietti, *Nat. Mater.*, 2009, **8**, 76–80.

21 J. Liu, Y. Liu, N. Liu, Y. Han, X. Zhang, H. Huang, Y. Lifshitz, S. T. Lee, J. Zhong and Z. Kang, *Science*, 2015, **347**, 970–974.

22 R. S. Sprick, J. X. Jiang, B. Bonillo, S. Ren, T. Ratvijitvech, P. Guiglion, M. A. Zwijnenburg, D. J. Adams and A. I. Cooper, *J. Am. Chem. Soc.*, 2015, **137**, 3265–3270.

23 L. Li, Z. Cai, Q. Wu, W. Y. Lo, N. Zhang, L. X. Chen and L. Yu, *J. Am. Chem. Soc.*, 2016, **138**, 7681–7686.

24 C. Yang, B. C. Ma, L. Zhang, S. Lin, S. Ghasimi, K. Landfester, K. A. I. Zhang and X. Wang, *Angew. Chem., Int. Ed.*, 2016, **55**, 9202–9206.

25 J. S. M. Lee and A. I. Cooper, *Chem. Rev.*, 2020, **120**, 2171–2214.

26 R. S. Sprick, Y. Bai, A. A. Y. Guilbert, M. Zbiri, C. M. Aitchison, L. Wilbraham, Y. Yan, D. J. Woods, M. A. Zwijnenburg and A. I. Cooper, *Chem. Mater.*, 2019, **31**, 305–313.

27 V. S. Mothika, P. Sutar, P. Verma, S. Das, S. K. Pati and T. K. Maji, *Chem.–Eur. J.*, 2019, **25**, 3867–3874.

28 V. S. Vyas, F. Haase, L. Stegbauer, G. Savasci, F. Podjaski, C. Ochsenfeld and B. V. Lotsch, *Nat. Commun.*, 2015, **6**, 8508.

29 E. Jin, Z. Lan, Q. Jiang, K. Geng, G. Li, X. Wang and D. Jiang, *Chem*, 2019, **5**, 1632–1647.

30 S. Wei, F. Zhang, W. Zhang, P. Qiang, K. Yu, X. Fu, D. Wu, S. Bi and F. Zhang, *J. Am. Chem. Soc.*, 2019, **141**, 14272–14279.

31 J. Thote, H. B. Aiyappa, A. Deshpande, D. Díaz Díaz, S. Kurungot and R. Banerjee, *Chem.–Eur. J.*, 2014, **20**, 15961–15965.

32 L. Li, Z. Zhou, L. Li, Z. Zhuang, J. Bi, J. Chen, Y. Yu and J. Yu, *ACS Sustain. Chem. Eng.*, 2019, **7**, 18574–18581.

33 A. F. M. EL Mahdy, A. M. Elewa, S. W. Huang, H. H. Chou and S. W. Kuo, *Adv. Opt. Mater.*, 2020, **8**, 2000641.

34 W. Huang, Q. He, Y. Hu and Y. Li, *Angew. Chem., Int. Ed.*, 2019, **58**, 8676–8680.

35 L. Guo, Y. Niu, H. Xu, Q. Li, S. Razzaque, Q. Huang, S. Jin and B. Tan, *J. Mater. Chem. A*, 2018, **6**, 19775–19781.

36 L. Guo, Y. Niu, S. Razzaque, B. Tan and S. Jin, *ACS Catal.*, 2019, **9**, 9438–9445.

37 M. Liu, Q. Huang, S. Wang, Z. Li, B. Li, S. Jin and B. Tan, *Angew. Chem., Int. Ed.*, 2018, **57**, 11968–11972.

38 D. Kong, X. Han, J. Xie, Q. Ruan, C. D. Windle, S. Gadipelli, K. Shen, Z. Bai, Z. Guo and J. Tang, *ACS Catal.*, 2019, **9**, 7697–7707.

39 C. B. Meier, R. Clowes, E. Berardo, K. E. Jelfs, M. A. Zwijnenburg, R. S. Sprick and A. I. Cooper, *Chem. Mater.*, 2019, **31**, 8830–8838.

40 R. S. Sprick, B. Bonillo, R. Clowes, P. Guiglion, N. J. Brownbill, B. J. Slater, F. Blanc, M. A. Zwijnenburg, D. J. Adams and A. I. Cooper, *Angew. Chem., Int. Ed.*, 2016, **55**, 1824–1828.

41 X. Wang, L. Chen, S. Y. Chong, M. A. Little, Y. Wu, W. H. Zhu, R. Clowes, Y. Yan, M. A. Zwijnenburg, R. S. Sprick and A. I. Cooper, *Nat. Chem.*, 2018, **10**, 1180–1189.

42 Z. Wang, X. Yang, T. Yang, Y. Zhao, F. Wang, Y. Chen, J. H. Zeng, C. Yan, F. Huang and J. X. Jiang, *ACS Catal.*, 2018, **8**, 8590–8596.

43 C. Cheng, X. Wang and F. Wang, *Appl. Surf. Sci.*, 2019, **495**, 143537.

44 X. Gao, C. Shu, C. Zhang, W. Ma, S. B. Ren, F. Wang, Y. Chen, J. H. Zeng and J. X. Jiang, *J. Mater. Chem. A*, 2020, **8**, 2404–2411.

45 J. Wang, G. Ouyang, Y. Wang, X. Qiao, W. S. Li and H. Li, *Chem. Commun.*, 2020, **56**, 1601–1604.

46 M. V. Ivanov, K. Thakur, A. Boddeda, D. Wang and R. Rathore, *J. Phys. Chem. C*, 2017, **121**, 9202–9208.

47 J. X. Jiang, A. Trewin, D. J. Adams and A. I. Cooper, *Chem. Sci.*, 2011, **2**, 1777–1781.

48 W. Y. Huang, Z. Q. Shen, J. Z. Cheng, L. L. Liu, K. Yang, X. Chen, H. R. Wen and S. Y. Liu, *J. Mater. Chem. A.*, 2019, **7**, 24222–24230.

49 Z. A. Lan, W. Ren, X. Chen, Y. Zhang and X. Wang, *Appl. Catal. B.*, 2019, **245**, 596–603.

50 M. Sachs, H. Cha, J. Kosco, C. M. Aitchison, L. Francàs, S. Corby, C. L. Chiang, A. A. Wilson, R. Godin, A. Fahey-Williams, A. I. Cooper, R. S. Sprick, I. McCulloch and J. R. Durrant, *J. Am. Chem. Soc.*, 2020, **142**, 14574–14587.

51 J. Kosco and I. McCulloch, *ACS Energy Lett*, 2018, **3**, 2846–2850.

52 Z. Hu, X. Zhang, Q. Yin, X. Liu, X.-f. Jiang, Z. Chen, X. Yang, F. Huang and Y. Cao, *Nano Energy*, 2019, **60**, 775–783.

53 T. Simon, N. Bouchonville, M. J. Berr, A. Vaneski, A. Adrović, D. Volbers, R. Wyrwich, M. Döblinger, A. S. Susha, A. L. Rogach, F. Jäckel, J. K. Stolarczyk and J. Feldmann, *Nat. Mater.*, 2014, **13**, 1013–1018.

54 Y. Zhao, W. Ma, Y. Xu, C. Zhang, Q. Wang, T. Yang, X. Gao, F. Wang, C. Yan and J. X. Jiang, *Macromolecules*, 2018, **51**, 9502–9508.

55 M. Schwarze, D. Stellmach, M. Schröder, K. Kailasam, R. Reske, A. Thomas and R. Schomäcker, *Phys. Chem. Chem. Phys.*, 2013, **15**, 3466–3472.

56 S. Bernhardt, M. Kastler, V. Enkelmann, M. Baumgarten and K. Müllen, *Chem.–Eur. J.*, 2006, **12**, 6117–6128.

57 X. Wang and M. Wang, *Polym. Chem.*, 2014, **5**, 5784–5792.